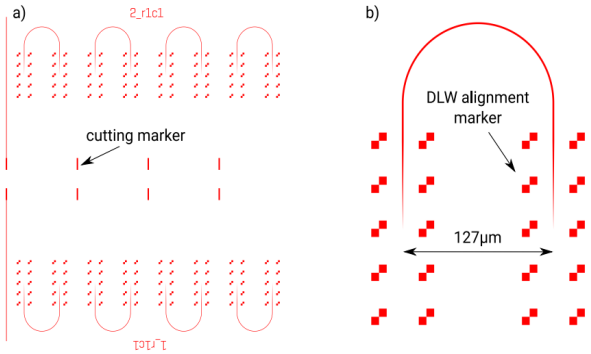

Figure 3.1: a) The general planar circuitry design used for characterizing coupling efficiency and b) an individual device.

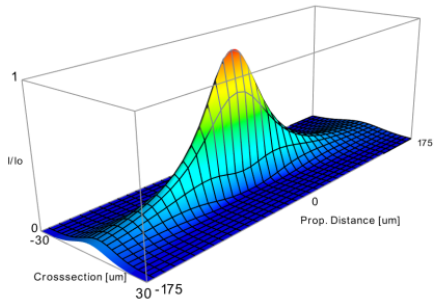

Figure 7: Regularly-spaced elevation plot of crossections of the WPM simulation results of a Gaussian input. Height and color both resemble intensity for better visualisation.

through an overlap integral. The Gaussian overlap integral G_{AB} of an array A and its corresponding best-fit array B over the volume V is calculated by

$$G_{AB} = \frac{|\int A \cdot B \, dV|^2}{\int |A|^2 \cdot |B|^2 dV}. \tag{3.3}$$

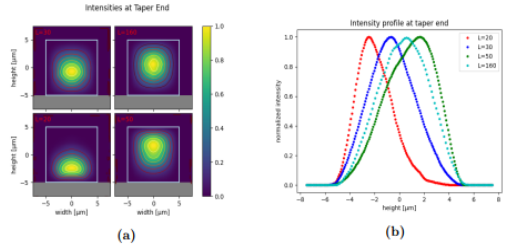

Figure 6: Meep simulations of tapers with lengths of $L = 20\,\mu m$, $L = 30\,\mu m$, $L = 50\,\mu m$ and $L = 160\,\mu m$. In (a) the normalised intensity at the end of the tapers is plotted. The light blue frame is a reference to indicate the tapers boundaries and the grey areas resemble the substrate. Added is a differently coloured contour plot to further enhance the visualisation of the modes geometry. In (b) the central vertical profiles of the different distributions are plotted.

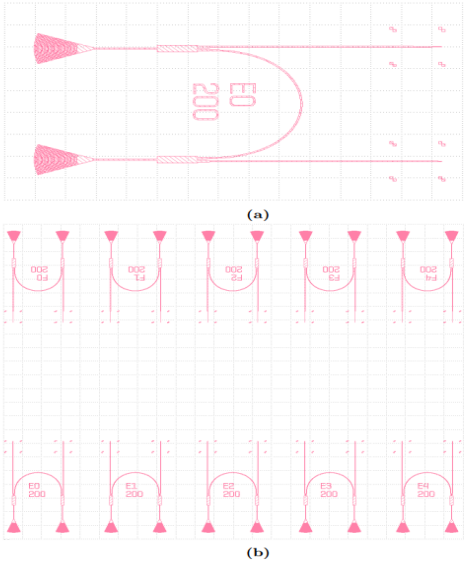

Figure 17: Design of the nanophotonic structures. One unit contains two grating couplers, each leading to a MMI where the inner arm of the two connects the two, leading half of the light back to the other grationg coupler, while the other arm connects to a taper (a). This taper is the port for the direct-laser-writing components that are printed in a later step. These units are arranged in rows with opposing directions (b). After fabrication it is possible to cut the chip in the gap between the two rows to create a clean edge at a desired distance from the port.